Effect of Chlorin Structure on Theoretical Electronic Absorption Spectra and on the Energy Released by Porphyrin-Based Photosensitizers

Marcela Palma,[†] Gloria I. Cárdenas-Jirón,*[,†] and M. Isabel Menéndez Rodríguez*[,‡]

Laboratorio de Química Teórica, Departamento de Ciencias del Ambiente, Facultad de Química y Biología, Universidad de Santiago de Chile, USACH Casilla 40, Correo 33, Santiago, Chile, and Departamento de Química Física y Analítica, Facultad de Química. Universidad de Oviedo, C/Julián Clavería 8, 33006 Oviedo, Asturias, Spain

Received: May 16, 2008; Revised Manuscript Received: September 10, 2008

In this work eight porphyrins (**p**) and eight chlorins (**c**) are theoretically characterized [BLYP/6-31G(d)] in their singlet and triplet states. Nine of them ($\mathbf{1_p}$, $\mathbf{1_c}$, $\mathbf{2_p}$, $\mathbf{3_p}$, $\mathbf{4_p}$, $\mathbf{5_p}$, $\mathbf{6_c}$, $\mathbf{7_c}$, and $\mathbf{8_c}$) have already been synthesized and are in trial use in photodynamic therapy (PDT). The seven remaining were built up as chlorins analogous to porphyrins $\mathbf{2_p}-\mathbf{5_p}$ and porphyrins analogous to chlorins $\mathbf{6_c}-\mathbf{8_c}$. The aim is to investigate the effect of the chlorin structure on the Q-band of electronic spectra at BLYP/6-31G(d) (gas phase, methanol solution) and at BHANDHLYP/6-31+G(d) (methanol solution), and on the triplet → singlet energy emission, as these two factors determine the quality of a good photosensitizer. It is found that *meso* substituents lead to greater geometry distortions than β-substituents in both porphyrins and chlorins and in both singlet and triplet states. In methanol solution, chlorin-like structures with β substitution present significantly red-shifted Q-bands in comparison with their porphyrin analogues, so they would be better photosensitizers than porphyrins. Concerning to the triplet → singlet energy emission calculated in methanol solution, three porphyrins ($\mathbf{4_p}$, $\mathbf{6_p}$, and $\mathbf{8_p}$) and all the studied substituted chlorins could be useful to generate active $^1O_2$. $\mathbf{4_c}$ would be the best photosensitizer, as it absorbs the largest wavelength in the therapeutic window (approximately 690 nm) and releases the amount of energy closest to the required one (1.22 eV).

1. Introduction

Porphyrin and its derivatives are widely studied due to their photophysical and electrochemical properties. They have been used as sensors and catalysts and have been applied in nonlinear optics.[1−3] The feature we wish to explore in this work is their ability as photosensitizers, which could be used in photodynamical therapy (PDT) for the treatment of cancer and other diseases.[4−6]

Because porphyrins are chromophores, they absorb light at visible wavelength, producing a singlet excited state that decays to the first triplet excited state. This last state transfers its energy to molecular oxygen ($^3O_2$) present in the medium, generating the singlet excited oxygen ($^1O_2$), which is responsible for the death of ill cells.[7] At the experimental level, much work has been performed to look for the best photosensitizers.[7−17] From a chemical viewpoint, one of the criteria that have to be fulfilled is the ability of the photosensitizer to absorb in the therapeutic window, that is, between 600 and 800 nm. Light in this spectral region is scattered to a relatively small extent by most mammalian tissues and is poorly absorbed by endogenous chromophores such as melanin, cytochromes, and hemoglobin. As a consequence, red light possesses a high penetration power into human tissues and can be selectively absorbed by photosensitizing agents localized in predetermined sites of the organism.[7] A wavelength up 800 nm (1.55 eV) is too weak to activate the photosensitizing derivative.[7] The absorption wavelength criterion itself is not enough, and it is also necessary that the photosensitizer has a good quantum yield for the first excited triplet state, which has to release the appropriate energy to yield singlet oxygen, that is, 0.95 eV (22.0 kcal/mol) or greater.[10] This value is the minimum energy necessary to excite the triplet ground state of molecular oxygen ($^3O_2$) to its first excited singlet state ($^1O_2$) of lower energy, named as $^1\Delta_g$. The next excited singlet state of molecular oxygen corresponds to state $^1\Sigma_g^+$, with excitation energy of 1.63 eV (37.5 kcal/mol). Although both $^1\Delta_g$ and $^1\Sigma_g^+$ are significant in the gas phase, only the $^1\Delta_g$ state is important in condensed phase. From a biological viewpoint, aspects such as biolocalization of the photosensitizers (mitocondria, liposomes, etc.), formation of aggregates, efficiency, and skin photosensibility are being studied,[4−6,18−20] to mention but a few. Several interesting theoretical works have been published recently,[21−26] which study the absorption spectra of some photosensitizers proposed in the literature, but there are still other aspects that need to be investigated: for instance, how the position (*meso*, β) and type of substituents and the change from a porphyrin-like compound to chlorin affect the photosensitizing capability of the molecules. On the basis of the knowledge acquired, new families of porphyrins should be theoretically analyzed and characterized in order to find better photosensitizers.

In this work we consider a set of porphyrin derivatives with different peripheral substituents at β and *meso* positions. Some of them are actually used as drugs in PDT, and other are in clinical trials. As a reference we also considered the unsubstituted porphyrin $\mathbf{1_p}$. The selected molecules are two types of hematoporphyrins [a photofrin-related derivative[10] ($\mathbf{2_p}$) and protoporphyrin IX ($\mathbf{3_p}$, levulan)[27]], a benzoporphyrin derivative ($\mathbf{4_p}$, visudyne),[28] and tetrasulfonated *meso*-tetraphenyl porphyrin ($\mathbf{5_p}$, H_2TPPS_4).[29] As is well-known, a chlorin can be considered

* Authors to whom correspondence should be addressed: e-mail gloria.cardenas@usach.cl (G.I.C.-J.) or isabel@uniovi.es (M.I.M.R.).
† Universidad de Santiago de Chile.
‡ Universidad de Oviedo.

10.1021/jp804350n CCC: $40.75
Published on Web 11/24/2008

SCHEME 1: Atom Numbering and Substituents Used for Porphyrin and Chlorin Derivatives

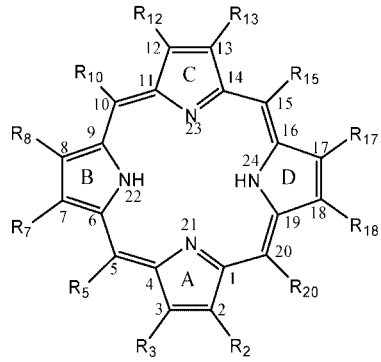

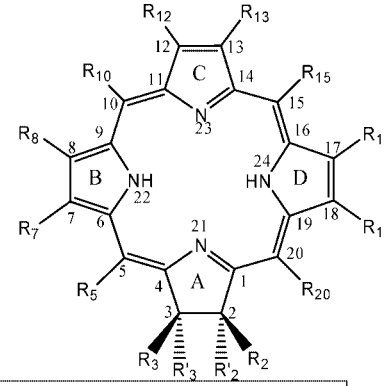

Molecules	Positions	substituents
2_p/2_c	R_2, R_{18}	-CH_2-CH_2-COOH
	R_8, R_{13}	-CHOH-CH_3
	R_3, R_7, R_{12}, R_{17}	-CH_3
3_p/3_c	R_2, R_{18}	-CH_2-CH_2-COOH
	R_8, R_{13}	-CH=CH_2
	R_3, R_7, R_{12}, R_{17}	-CH_3
4_p/4_c	R_2, R_{18}	-CH_2-CH_2-$COOCH_3$
	R_{12} - R_{13}	-CH=CH-C($COOCH_3$)- C($COOCH_3$)-
	R_7	-CH=CH_2
	R_3, R_8, R_{13}, R_{17}	-CH_3
5_p/5_c	R_5, R_{10}, R_{15}, R_{20}	-C_6H_4-SO_3H
6_p/6_c	R_5, R_{10}, R_{15}, R_{20}	-C_6H_4-OH
7_p/7_c	R_2	-CH_2-CO-NH-CHCOOH-CH2-COOH
	R_{18}	-COOH
	R_8	-CH=CH_2
	R_{13}	-CH_2-CH_3
	R_3, R_7, R_{12}, R_{17}	-CH_3
	R_{20}	-CH_2-COOH
8_p/8_c	R_2	-CH_2-CH_2-COOH
	R_{18}	-COOH
	R_8	-CH=CH_2
	R_{13}	-CH_2-CH_3
	R_3, R_7, R_{12}, R_{17}	-CH_3
	R_{20}	-COOH

a porphyrin derivative in which a double bond between two β-carbon atoms of a pyrrole ring has been reduced. Unsubstituted chlorin absorbs longer wavelengths in the therapeutic window than porphyrin, so it seems to be more appropriate for use in PDT. For this reason we theoretically tried to predict the photosensitizing characteristics of chlorin molecules analogous to the porphyrin derivatives just mentioned. In addition, the chlorins commercially known as foscan (**6_c**),[30,31] mace-e6 chlorin (**7_c**),[32] and p6 chlorin (**8_c**),[33] are included in this study, along with the isolated chlorin (**1_c**) taken as a reference. We shall theoretically test, as well, how their porphyrin analogues fulfill the criteria to be good photosensitizers. Thus, a total of 16 molecules will be considered.

The aim of this work is to rationalize, from a theoretical viewpoint by use of quantum chemistry, how the presence of different substituents and/or a chlorin structure affect the photosensitizing capability of the molecules, that is, the location of the Q-band (the lowest energy band of a UV−vis spectrum, which corresponds to the formation of the first singlet excited state), and the energy released in the deactivation of the photosensitizing agent.

2. Computational Aspects

A full geometry optimization without symmetry constraints was performed for the molecules under study at B3LYP/6-31G(d) computational level[34] by use of the Jaguar 6.0 package,[35] in both their singlet ground states and first triplet excited states. The latter were calculated with the default method of Jaguar 6.0 at Restricted Open B3LYP level to avoid spin contamination. A frequency calculation was carried out for each molecule to check that the optimized geometry corresponded to an energy minimum, that is, with all frequency values positive. Singlet- and triplet-state energies were calculated in the gas phase and in methanol solution (dielectric constant of 32.6), as this is the solvent experimentally used for substituted molecules considered in this study. The solvent was modeled by use of the Poisson−Boltzmann solver as implemented in Jaguar 6.0.[36] The energy released in the triplet → singlet transition, ΔE_{TS}, of each porphyrin derivative was calculated as the difference between the energy of the structures with the corresponding spin multiplicity optimized with Jaguar 7.5 in the gas phase. ΔE_{TS} in methanol solution was calculated in the same way from single-point calculations on the gas-phase-optimized structures by use of the Poisson−Boltzmann solver.

The time-dependent density functional theory (TD-DFT) [37−39] formalism was used to calculate the electronic absorption spectra of the whole set of porphyrin and chlorin derivatives and was carried out with Gaussian03, revision D.01.[40] Singlet−singlet electronic transitions were calculated as vertical excitations, and only one-electron excitations between these states were studied.

TABLE 1: Dihedral Angles[a] for Optimized Ground State and First Triplet Excited State of Porphyrin and Chlorin Derivatives

	$\angle C_1N_{21}N_{23}C_{14}$	$\angle C_1N_{21}N_{23}C_{11}$	$\angle C_6N_{22}N_{24}C_{19}$	$\angle C_6N_{22}N_{24}C_{16}$
$\mathbf{1_p}/\mathbf{1_c}$ singlet	0.01/1.45	−179.87/−178.45	0.05/−0.69	179.91/178.98
$\mathbf{1_p}/\mathbf{1_c}$ triplet	0.00/1.59	179.98/−178.43	0.05/−0.80	180.0/179.11
$\mathbf{2_p}/\mathbf{2_c}$ singlet	2.14/7.57	−176.37/−171.22	3.41/−2.60	176.96/173.43
$\mathbf{2_p}/\mathbf{2_c}$ triplet	4.12/7.02	−176.56/−169.03	2.45/−3.39	176.47/168.21
$\mathbf{3_p}/\mathbf{3_c}$ singlet	0.25/4.91	177.11/−170.39	−0.52/−4.80	176.79/171.26
$\mathbf{3_p}/\mathbf{3_c}$ triplet	−0.88/2.52	−179.55/−172.09	−0.10/−3.24	177.57/167.79
$\mathbf{4_p}/\mathbf{4_c}$ singlet	−4.87/−12.27	173.82/163.74	5.60/10.04	−175.28/−171.54
$\mathbf{4_p}/\mathbf{4_c}$ triplet	0.55/−11.66	177.61/163.34	2.37/11.19	178.03/−170.30
$\mathbf{5_p}/\mathbf{5_c}$ singlet	6.37/−4.81	−174.72/175.10	2.06/10.29	173.00/−174.37
$\mathbf{5_p}/\mathbf{5_c}$ triplet	12.70/−8.11	−166.09/173.93	2.41/13.66	168.57/−175.80
$\mathbf{6_p}/\mathbf{6_c}$ singlet	−14.36/−19.28	158.40/154.11	14.42/19.96	−159.37/−154.90
$\mathbf{6_p}/\mathbf{6_c}$ triplet	−19.20/−25.67	148.82/139.22	17.92/26.26	−146.43/−136.96
$\mathbf{7_p}/\mathbf{7_c}$ singlet	0.43/−1.78	−172.11/−171.84	14.57/12.80	−179.81/178.54
$\mathbf{7_p}/\mathbf{7_c}$ triplet	0.24/6.49	−169.96/−165.44	23.40/14.08	−173.56/170.18
$\mathbf{8_p}/\mathbf{8_c}$ singlet	1.66/−1.73	−171.29/−176.59	15.07/10.12	−179.74/176.18
$\mathbf{8_p}/\mathbf{8_c}$ triplet	−0.64/14.94	−170.47/−161.36	25.81/8.63	179.44/158.21

[a] Dihedral angles are given in degrees and were calculated at B3LYP/6-31G(d) level. The first value corresponds to porphyrins and the second to chlorins.

Modeling of the solvent was done with the CPCM method,[41] which performs the PCM (polarizable continuum model) method by use of a conductor like polarized medium, and the simple united atom topological model (UA0) to describe the atomic radii. To choose the adequate theory level to calculate the electronic spectra of the whole set of porphyrins and chlorins, we tested seven different exchange correlation functionals and augmented the basis set with diffuse functions on heavy atoms [6-31+G(d)] for unsubstituted porphyrin, $\mathbf{1_p}$, and chlorin, $\mathbf{1_c}$. Results for the Q-band, that of lowest energy, for these compounds calculated in methanol solution are shown and discussed in section 3.2, where we also analyze previous theoretical results available in the literature and calculated at different computational levels. Trying to get theoretical Q-bands closer to experimental ones, we also tested the influence of two molecules of solvent considered explicitly and calculated these complexes with the CPCM model, as will be seen in section 3.2.1.

3. Results and Discussion

3.1. Ground-State Molecular Structures. Optimized molecular structures for the ground-state porphyrins and chlorins can be described on the basis of Scheme 1 and Table 1 (see Supporting Information for explicit drawing and coordinates of each optimized molecule and also for the interatomic distances). As a quantitative measure of the planarity of the core of the macrocycles, we considered the four dihedral angles collected in Table 1: $\angle C_1N_{21}N_{23}C_{14}$ and $\angle C_1N_{21}N_{23}C_{11}$, referring to the opposite pyrrole rings A and C, and $\angle C_6N_{22}N_{24}C_{19}$ and $\angle C_6N_{22}N_{24}C_{16}$, referring to pyrrole rings B and D. (See Scheme 1 for atom numbering.)

$\mathbf{1_p}$, porphyrin, is planar, as the greater deviation corresponds to $\angle C_1N_{21}N_{23}C_{11}$ and it is only 0.13° toward the lower part of the mean macrocycle plane. $\mathbf{1_c}$, chlorin, can also be considered essentially planar, although dihedral angles affecting rings A (where C=C reduction has taken place) and C show more deviation with values of 1.45° and −178.45°. β-Substituents in $\mathbf{2_p}$, photofrin, and $\mathbf{3_p}$, levulan (see Scheme 1), provoke small alterations of planarity, a little greater for $\mathbf{2_p}$ (between 2.14° and −176.37°), which has a secondary alcohol at R_8 and R_{13}, instead of the vinyl group of $\mathbf{3_p}$ (planarity deviations between 0.25° and 176.79°). $\mathbf{2_c}$ and $\mathbf{3_c}$ are more distorted than their corresponding porphyrins with dihedral angles in the range of −2.60° to −170.39°. As expected, β-carbon atoms C_2 and C_3, mainly C_2, are clearly displaced from the mean molecular plane in these chlorins.

Visudyne structures $\mathbf{4_p}$ and $\mathbf{4_c}$ have in β-positions methyl and vinyl groups, ester chains, and a 6-membered cycle merged to the C pyrrole ring. In fact, C_{13} has sp^3 hybridation to be able to form four bonds. As a consequence, $\mathbf{4_p}$ and $\mathbf{4_c}$ show the largest deviations from planarity among all the β-substituted molecules, mainly $\mathbf{4_c}$, for which $\angle C_1N_{21}N_{23}C_{11}$ becomes 163.74°.

Four phenyl substituents at *meso* C atoms affect the planarity of the macrocycle to a larger extent than β substituents. Their influence seems to depend on the orientation of the phenyl rings and on the position of the functional group at the phenyl ring, which also determine the steric repulsions with β C atoms of the pyrrole rings. If phenyl rings flanking pyrrole rings A and C, say, push them downward, the B and D rings are lifted upward and the molecule adopts a wave conformation, which is more pronounced in $\mathbf{6_p}$ and $\mathbf{6_c}$.

Compounds **7** and **8** present only one aliphatic acidic chain at *meso*-C_{20}, and they differ from each other in this acid group and in the R_2 substituent (see Scheme 1). The four compounds present quite distorted macrocycles due to dihedral angles $\angle C_1N_{21}N_{23}C_{11}$ and $\angle C_6N_{22}N_{24}C_{19}$, which have values similar to those for 4-fold *meso*-substituted derivatives.

For porphyrins $\mathbf{1_p}-\mathbf{6_p}$ and chlorins $\mathbf{1_c}-\mathbf{6_c}$ (except $\mathbf{4_c}$), the distances between opposite *meso*-C atoms, rC5···C15 and rC10···C20, are practically the same, and their values are between 6.84 and 6.92 Å. For $\mathbf{4_c}$ the difference between rC5···C15 and rC10···C20 amounts to 0.13 Å. The macrocycle of $\mathbf{7_p}$, $\mathbf{7_c}$, $\mathbf{8_p}$, and $\mathbf{8_c}$ is less symmetric, as the presence of one acid chain at *meso*-C_{20} enlarges the rC10···C20 distance and rC5···C15 becomes shorter. The difference between both distances is 0.34 Å for $\mathbf{7_c}$ and $\mathbf{8_c}$, 0.47 Å for $\mathbf{8_p}$, and 0.60 Å for $\mathbf{7_p}$. The distances between N21 and N23, those N atoms without bonded H atoms, are smaller than N22−N24 distances for all of the molecules except for $\mathbf{4_c}$.

Concerning molecular structures of the ground state, it can be concluded that the N21−N23 distance is smaller than N22−N24 distance for all of the studied molecules. β-Substituents diminish the macrocycle planarity, but four *meso*-phenyl groups produce an augmented distortion of the macrocycle. Molecules with β and C_{20} substituents show greater twisting in the pyrrole rings surrounding the *meso*-acid chain. β, and tetraphenyl *meso*-substituted derivatives have quite similar distances among opposite *meso*-C atoms, but when only one

TABLE 2: Lowest Singlet Excitation Energies Associated with Q-band for Free Base Porphyrin $\mathbf{1_p}$ and Chlorin $\mathbf{1_c}$ Obtained by Different Theoretical Methods, Along with Experimental Data[a]

method of calculation[b]	porphyrin ($\mathbf{1_p}$)	ref	chlorin ($\mathbf{1_c}$)	ref
	Correlated ab Initio Methods			
SAC-CI	1.81 (9.6%)	47	1.68 (15.2%)	50
SAC-CI	1.77 (11.6%)	49	1.64 (−17.2%)	61
SAC-CI	1.75 (12.6%)	51		
SAC-CI	1.75 (12.6%)	53		
SAC-CI	1.88 (6.1%)	61		
SAC-CI	1.70 (15.2%)	49		
CIS	2.48 (−24.2%)	52		
CIS	2.56 (−28.3%)	58		
CIS	2.41 (−20.7%)	38		
RPA, SVP	1.72 (14.1%)	38		
CASPT2	1.63 (18.7%)	48		
CASPT2	1.20 (40.4%)	54		
CASPT2	1.70 (15.2%)	56		
STEOM-CC	1.75 (12.6%)	50		
STEOM-CC	1.72 (14.1%)	52		
STEOM-PT	2.20 (−10.1%)	52		
CS INDO CI	2.14 (−7.1%)	55		
MRCI	1.97 (−1.5%)	57	2.46 (−24.2%)	60
MRMP	1.63 (18.7%)	62	1.77 (10.6%)	62
INDO/S CIS	1.70 (15.2%)	59		
INDO/S RPA	1.46 (27.3%)	59		
SCF-CI	2.27 (−13.6%)	60		
	Methods Combining DFT and Correlated ab Initio Methods			
DFT/MRCI BHLYP,VDZP	1.94 (3.0%)	43		
DFT/MRCI BHLYP	1.94 (3.0%)	45	1.99 (−0.5%)	43
DFT/CIS B3LYP, VDZP	2.03 (−1.5%)	44	2.09 (−5.6%)	44
CASSCF			2.76 (−39.4%)	62
	TD-DFT (from Literature)			
TD-DFT B-P, SVP + diff	2.13 (−6.6%)	42		
TD-DFT B-P, SVP	2.13 (−6.6%)	42		
	2.17 (−8.6%)	53		
TD-DFT B-P, TZVP	2.13 (−6.6%)	42		
DFT B-P, TZ2P STO	2.16 (−8.1%)	46		
TD-DFT B3LYP, SVP	2.24 (−12.1%)	42		
	2.27 (−13.6%)	38		
TD-DFT PBE0 6-31+G(d)	2.36 (−16.8%)[c]	25	2.25 (−13.6%)[d]	25
TD-DFT S-VWN, SVP	2.18 (−9.1%)	38		
	TD-DFT (This Work)[e]			
TD-DFT BLYP/6-31G(d)	2.19 (−9.6%)		2.21 (−11.6%)	
TD-DFT BPW91/6-31+G(d)	2.21 (−10.6%)		2.21 (−11.6%)	
TD-DFT PBE0/6-31+G(d)	2.21 (−10.6%)		2.21 (−11.6%)	
TD-DFT B3LYP/6-31+G(d)	2.30 (−15.2%)		2.27 (−14.6%)	
TD-DFT PBE1/6−31+G(d)	2.33 (−16.7%)		2.29 (−15.7%)	
TD-DFT BHANDH/6-31+G(d)	2.34 (−17.2%)		2.25 (−13.6%)	
TD-DFT BHANDHLYP/6-31+G(d)	2.29 (−14.6%)		2.22 (−12.1%)	
experimental	2.02[c]	63	1.98[f]	60

[a] Energies are given in electronvolts; relative errors are given in parentheses. [b] SAC, symmetry-adapted cluster; RPA, random phase approximation; STEOM, similarity-transformed equation of motion. [c] Measured in ethanol. [d] Calculated in water [e] This work, in methanol solution. [f] Measured in benzene.

meso substituent is present, the diagonal affecting this *meso*-C atom becomes longer.

3.2. Ground-State Activation: $S_0 \rightarrow S_1$. ***3.2.1. Free Base Porphyrin and Chlorin Electronic Absorption Spectra.*** In order to calculate the Q-band of the electronic absorption spectra of substituted porphyrins and chlorins studied in this work, we previously tested seven exchange correlation functionals for $\mathbf{1_p}$ and $\mathbf{1_c}$. Results are shown in Table 2, where we also included values obtained with other theoretical methods available in the literature.[42−63]

Since the electronic spectra of large aromatic molecules, such $\mathbf{1_p}$ and $\mathbf{1_c}$, have become tractable for correlated ab initio calculations, several studies have appeared, as shown in Table 2. Overall, results obtained al these levels present large relative errors. It is known that for large molecules the quality of correlated ab initio calculations is negatively influenced by the necessity to compromise on the quality of the basis set and the magnitude of active space that can be employed (CASPT2) or the number of determinants that can be taken into account in the CI. Among the results collected in Table 2 performed with correlated ab initio methods, MRCI yields the best Q-band for $\mathbf{1_p}$ (1.97 eV, compared with the experimental value 2.02 eV), but this method seems to fail in the description of the Q-band of $\mathbf{1_c}$ (24.2% relative error). On the other hand, previous studies[38] have shown that excitation energies obtained at the TD-DFT level are in much better agreement with experimental values than those obtained at CIS level. Table 2 clearly shows that the best theoretical Q-bands for both $\mathbf{1_p}$ and $\mathbf{1_c}$ are those obtained

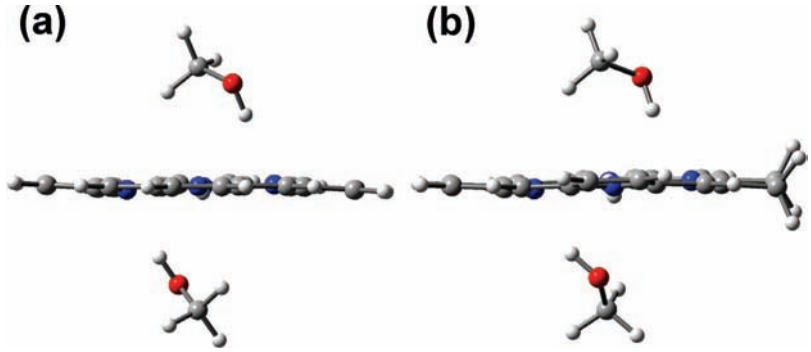

Figure 1. Optimized molecular structure of (a) $\mathbf{1_p}$ and (b) $\mathbf{1_c}$ with explicit methanol solvent, calculated at B3LYP/6-31G(d) level.

with methods combining DFT and correlated ab initio methods, both including only single excitations (CIS)[44] or performing a multireference CI (MRCI) treatment,[43,45] but they are too computer-demanding for systems as large as those in the present work. Results obtained with TD-DFT indicate that for most low-lying excitation energies the double-ζ+ polarization basis sets seem satisfactory.[42] Although we could not find TD-DFT results in the literature for $\mathbf{1_c}$, it can be seen that results obtained for $\mathbf{1_p}$ with recently created functionals and default basis sets in Gaussian03 render errors slightly larger than those obtained with Karlsruhe basis sets.[42]

From the results obtained in this work it can be seen that BLYP, BPW91, and PBE0 yield the smallest errors in the Q-band energy, 9.6−10.6% and 11.6% for $\mathbf{1_p}$ and $\mathbf{1_c}$, respectively. On the other hand, B3LYP, PBE1, BHAND, and BHANDHLYP render greater errors in the Q-band for both molecules, 14.6−17.2% for $\mathbf{1_p}$ and 12.1−15.7% for $\mathbf{1_c}$. Even though these last functionals reproduce the experimental fact of the shorter energy (longer wavelength) absorption of chlorin, BHANDHLYP was the functional yielding the smaller error in the calculated value. We also calculated 10 singlet−singlet excitations with these seven functionals in methanol solution to compare them with the experimental values (results are shown in Supporting Information). We found that BLYP predicts the three lowest experimental bands with the smallest error, and B3LYP and BHANDHLYP present similar values but those obtained with the latter are slightly closer to the experimental values.

We also wondered if specific interactions between the porphyrin derivatives and solvent could affect their electronic spectra. In such a case, consideration of the solvent just as a continuum could be inadequate, so we performed a full optimization of $\mathbf{1_p}$ and $\mathbf{1_c}$ in the presence of two molecules of methanol (see Figure 1) at B3LYP/6-31G(d) level. Two hydrogen bonds were formed between methanol and a pyrrolic nitrogen atom with distances of ≈2.1 Å. Then a TD-DFT calculation for $\mathbf{1_p}$ and $\mathbf{1_c}$ was carried out with BLYP/6-31G(d) and BHANDHLYP/6-31+G(d). Results (included in Supporting Information) show that BLYP results are improved for both $\mathbf{1_p}$ and $\mathbf{1_c}$, but whereas the $\mathbf{1_p}$ Q-band (596 nm) is improved by 30 nm, the $\mathbf{1_c}$ Q-band is improved by only 5 nm. On the other hand, BHANDHLYP produce slightly worse values for both model compounds. However, BHANDHLYP continues to reproduce the experimental trend, already observed with the CPCM model, of smaller energy Q-band for $\mathbf{1_c}$ than for $\mathbf{1_p}$.

On the basis of the above discussion, we calculated electronic spectra for the set of substituted porphyrins and chlorins at BLYP/6-31G(d) and BHANDHLYP/6-31+G(d) theory levels, using the CPCM model to take into account solvent effects.

3.2.2. Comparison between Theoretical and Experimental UV−Vis Spectra. UV−vis absorption spectra of the studied compounds present two main absorption bands, as occurs with porphyrin itself:[64] a lower energy band named Q-band, which usually is of low intensity, and a higher energy and more intense band called the B or Soret band. The main characteristic of these compounds is that their Q-bands, corresponding to the excitation from the ground state (S_0) to the first singlet excited state (S_1), are located near the red region of the spectra, which makes them potentially good photosensitizers (as mentioned above, a good photosensitizer absorbs in the region between 600 and 800 nm). The computed vertical excitation energies in methanol solution [BLYP/6-31G(d) and BHANDHLYP/6-31+G(d)] are presented in Table 3 and are compared with available experimental values for porphyrins $\mathbf{1_p}$−$\mathbf{5_p}$ and for chlorins $\mathbf{1_c}$ and $\mathbf{6_c}$−$\mathbf{8_c}$. For comparison, results obtained at BLYP/6-31G(d) level in the gas phase are included in Supporting Information.

We first discuss results in methanol solution, as experimental data were measured in this solution. Concerning porphyrins with β-substitution, $\mathbf{2_p}$−$\mathbf{4_p}$, both functionals yield wavelengths smaller than experimental ones and show that the absorption wavelengths increase in the same way as, experimental ones when going from $\mathbf{2_p}$ to $\mathbf{4_p}$. BLYP results are closer to experimental values, whereas BHANDHLYP has wavelengths errors of about 12% in the three porhyrins.

Experimental values are available for a porphyrin, $\mathbf{5_p}$, and a chlorin, $\mathbf{6_c}$, substituted with four phenyl derivarives at *meso*-carbon atoms. BLYP renders for $\mathbf{5_p}$ a wavelength for the Q-band, λ_Q, longer than the experimental one and BHANDHLYP gives a smaller value with quite small error (3.2%). For $\mathbf{6_c}$, both functionals render smaller wavelengths than the experimental value of λ_Q. Experimental data indicate that $\mathbf{5_p}$ absorbs at a shorter wavelength than its corresponding unsubstituted analogue, $\mathbf{1_p}$, whereas the opposite is true for $\mathbf{6_c}$ compared to $\mathbf{1_c}$. Neither BLYP nor BHANDHLYP can reproduce this trend for $\mathbf{5_p}$; the BHANDHLYP functional yields the closest value. On the contrary, both functionals adjust to the trend observed for $\mathbf{6_c}$.

The last group of chlorins for which experimental data are available, $\mathbf{7_c}$ and $\mathbf{8_c}$, have substituents at both β and *meso* positions. As we have just seen, β- and *meso*-substituents of chlorins considered in this work enlarge the value of λ_Q relative to $\mathbf{1_c}$. Experimental values for $\mathbf{7_c}$ and $\mathbf{8_c}$ are slightly longer than λ_Q for unsubstituted analogue $\mathbf{1_c}$. In the same way, theoretical wavelengths for the Q-band, which are smaller than the experimental ones, are longer than those theoretically obtained for unsubstituted models.

The comparison between theoretical and experimental Q-bands in methanol solution shows that each theoretical λ_Q is

TABLE 3: TD-DFT Excitation Energies and Oscillator Strengths[a]

	BLYP				BHANDHLYP			
E_{exp},[b] eV	E,[b] eV	f	transition[c]	coefficient	E,[b] eV	f	transition[c]	coefficient
			Porphyrin ($\mathbf{1_p}$)					
2.02 (613)[d]	2.19 (566) [9.6%]	0.0020	H − 1 → L + 1	0.43	2.29 (540) [14.6%]	0.0028	H − 1 → L	0.57
			H → L	0.53			H → L + 1	0.57
			Chlorin ($\mathbf{1_c}$)					
1.98 (626)[e]	2.21 (559) [11.6%]	0.0800	H → L	0.54	2.22 (558) [12.1%]	0.1621	H − 1 → L + 1	−0.41
			H − 1 → L + 1	0.40			H → L	0.65
			Photofrin-p ($\mathbf{2_p}$)					
1.97 (630)	2.15 (577)[b] [8.4%]	0.0002	H → L	0.45	2.24 (553) [12.2%]	0.0217	H − 1 → L	−0.37
			H → L + 1	−0.27			H − 1 → L + 1	−0.39
			H − 1 → L	−0.23			H → L	0.44
			H − 1 → L + 1	−0.38			H → L + 1	−0.41
			Photofrin-c ($\mathbf{2_c}$)					
	2.14 (578)	0.1310	H → L	0.55	2.15 (578)	0.2113	H − 1 → L + 1	−0.39
			H − 1 → L + 1	−0.37			H → L	0.66
			Levulan-p ($\mathbf{3_p}$)					
1.95 (635)	2.09 (593) [6.6%]	0.0020	H → L	−0.19	2.21 (560) [11.8%]	0.0283	H − 1 → L	−0.28
			H → L + 1	0.48			H-1 → L + 1	0.45
			H − 1 → L	−0.43			H → L	0.51
			H − 1 → L + 1	−0.14			H → L + 1	0.31
			Levulan-c ($\mathbf{3_c}$)					
	2.06 (601)	0.1430	H → L	0.55	2.11 (589)	0.2249	H − 1 → L + 1	0.38
			H − 1 → L + 1	−0.36			H → L	0.66
			Visudyne-p ($\mathbf{4_p}$)					
1.80 (690)	1.87 (660) [4.3%]	0.103	H → L	0.46	2.04 (609) [11.7%]	0.1769	H − 1 → L	0.11
			H → L + 1	−0.24			H − 1 → L + 1	−0.36
			H − 1 → L	−0.31			H − 1 → L + 2	0.12
			H − 1 → L + 1	−0.29			H → L	0.64
							H → L + 1	0.13
			Visudyne-c ($\mathbf{4_c}$)					
	1.79 (694)	0.2410	H → L	0.57	1.82 (682)	0.3360	H − 1 → L + 1	0.25
			H → L + 1	−0.12			H − 1 → L + 2	0.19
			H − 1 → L + 1	−0.22			H → L	0.67
			H − 1 → L + 2	−0.12				
			Tetrasulfo-p ($\mathbf{5_p}$)					
2.10 (590)	2.03 (612) [−3.7%]	0.0490	H → L + 1	0.54	2.17 (571) [3.2%]	0.0055	H − 1 → L	0.54
			H − 1 → L	0.38			H → L	0.10
							H → L + 1	0.57
			Tetrasulfo-c ($\mathbf{5_c}$)					
	2.09 (594)	0.0710	H → L	0.54	2.13 (581)	0.1749	H − 1 → L + 1	0.40
			H − 1 → L + 1	−0.39			H → L	0.65
			Foscan-p ($\mathbf{6_p}$)					
	1.99 (623)	0.0530	H → L	0.49	2.16 (575)	0.0146	H − 1 → L	0.37
			H → L + 1	0.26			H − 1 → L + 1	0.38
			H − 1 → L	0.15			H → L	0.44
			H − 1 → L + 1	−0.35			H → L+1	−0.40
			Foscan-c ($\mathbf{6_c}$)					
1.90 (652)	2.08 (596) [8.6%]	0.0750	H → L	0.41	2.14 (579) [11.2%]	0.1483	H − 1 → L + 1	0.41
			H → L + 1	0.27			H → L	0.64
			H − 1 → L	−0.35				
			H − 1 → L + 1	0.27				
			e6-p ($\mathbf{7_p}$)					
	2.04 (607)	0.0060	H → L	0.20	2.17 (572)	0.0514	H − 1 → L + 1	0.49
			H → L + 1	−0.46			H → L	0.61
			H − 1 → L	0.46				
			H − 1 → L + 1	0.12				
			e6-c ($\mathbf{7_c}$)					
1.90 (654)	2.03 (609) [6.9%]	0.1710	H → L	0.56	2.11 (587) [10.2%]	0.2583	H − 1 → L + 1	0.36
			H − 1 → L + 1	−0.35			H → L	0.65
			p6-p ($\mathbf{8_p}$)					
	2.03 (611)	0.0170	H − 1 → L	0.41	2.12 (586)	0.0976	H − 1 → L	−0.18
			H − 1 → L + 1	0.21			H − 1 → L + 1	0.43
			H → L	0.32			H → L	0.61
			H → L + 1	−0.38			H → L + 1	0.17
			p6-c ($\mathbf{8_c}$)					
1.88 (660)	2.03 (612) [7.3%]	0.1960	H → L	0.57	2.09 (593) [10.2%]	0.2901	H − 1 → L + 1	−0.33
			H − 1 → L + 1	−0.31			H → L	0.66

[a] Calculated at BLYP/6-31G(d) and BHANDHLYP/6-31+G(d) in the solution phase (methanol). Experimental excitation energies (E_{exp}) are also included. [b] Values in nanometers are included in parentheses. [c] One-electron excitations, with coefficients larger than 0.1 in a given electronic transition, are included. [d] Reference 63. [e] Reference 60.

smaller than its corresponding experimental one [except for $\mathbf{5_p}$ at BLYP/6-31G(d)]. The enlargement of λ_Q produced by β-substituents in porphyrin derivatives and by β and *meso* substituents in chlorins is also found theoretically.

On the other hand, gas-phase Q-bands for chlorin-like compounds, calculated at BLYP/6-31G(d) level, present larger errors than in solution, so solvent seems to be more relevant for this kind of molecules.

3.2.3. Chlorin Effect on Calculated Absorption Bands. Once we have tested the quality of our theoretical levels, we can use them to predict the Q-band of chlorins and porphyrins analogous to those experimentally studied. In Table 3 we collect, in addition to the energy and wavelength associated with the Q-band, the oscillator strength and the composition of the electronic transitions in terms of the molecular orbitals in methanol solution for the eight couples of molecules. Results obtained in the gas phase are included in Supporting Information.

For all the molecules in the gas phase, we found that the presence of a chlorin-like structure leads to a decrease in the wavelength of the Q-band with respect to a porphyrin-like structure except for $\mathbf{4_c}$ (visudyne chlorin). Solvent plays a significant role in λ_Q values, as this trend is not followed in solution. For molecules with substitution only in β-carbon positions, the chlorin-like structure ($\mathbf{2_c}-\mathbf{4_c}$) presents a higher value of λ_Q than for their corresponding porphyrin-like structures. BLYP/6-31G(d) yields only small increases, while BHANDHLYP/6-31+G(d) magnifies the effect.

For molecules with substitution in the four *meso* positions, λ_Q presents a lower value for $\mathbf{5_c}$ and $\mathbf{6_c}$ than for $\mathbf{5_p}$ and $\mathbf{6_p}$ at BLYP/6-31G(d) level but a higher one at BHANDHLYP/6-31+G(d) level. An analogous situation was found for $\mathbf{1_p}$ and $\mathbf{1_c}$, for which experimental values are available, and it made us use the BHANDHLYP functional, so we accept that the presence of a chlorin structure in molecules substituted at the four *meso*-C atoms will slightly increase the value of λ_Q in comparison with the corresponding porphyrin, although the effect might be small. Both functionals yield lower λ_Q for $\mathbf{7_p}$ and $\mathbf{8_p}$ than for their analogous chlorins, following the trend found for the remaining molecules.

Because experimental data are measured in methanol solution, the theoretical results to be taken into account must be those calculated in solution phase. In fact, analysis of the results of λ_Q obtained in both phases shows that gas-phase results are not appropriate and could lead to wrong conclusions. Our analysis concludes that the theoretical values of λ_Q calculated in methanol solution present desirable behavior in all the molecules with substitution at the β-carbons: *the Q-band of the substituted chlorin-like structure is significantly red-shifted with respect to the substituted porphyrin-like structure* [for instance, BHANDHLYP/6-31+G(d) λ_Q differences are 25, 29, and 73 nm for $\mathbf{2_c}/\mathbf{2_p}$, $\mathbf{3_c}/\mathbf{3_p}$, and $\mathbf{4_c}/\mathbf{4_p}$]. The effect of chlorin structures in molecules having substitutions in *meso* positions is also a red shift but much smaller [ranging between 4 nm for $\mathbf{6_c}/\mathbf{6_p}$ and 15 nm for $\mathbf{7_c}/\mathbf{7_p}$ at BHANDHLYP/6-31+G(d) level].

Concerning the first condition a good photosensitizer must fulfill, the absorbance in the therapeutic window close to the red region, compound $\mathbf{4_c}$, visudyne chlorin, can be considered the best candidate, as it absorbs at the largest wavelength in the therapeutic window.

3.2.4. Molecular Orbital Description of Q-Band. The composition in terms of the molecular orbitals (MO) associated with the electronic transition of the Q-band is also shown in Table 3 at both theory levels in solution phase. Results obtained in the gas phase are included in Supporting Information. We analyze the MOs in the gas phase for the set of substituted molecules for which experimental data are available ($\mathbf{2_p}-\mathbf{5_p}$ and $\mathbf{6_c}-\mathbf{8_c}$) as we have checked that they are very similar to those in methanol solution. Figure 2 shows the surfaces of the four molecular orbitals that participate in the electronic transitions corresponding to the Q-band. For all of the molecules, we found that these MOs correspond to the four Gouterman MOs. In an attempt to understand the characteristic bands of the porphyrin, i.e., Soret and Q-bands, Gouterman[65−67] proposed in the 1960s the four-orbital model to explain the absorption spectra of porphyrins. According to this model, the absorption bands in porphyrin systems arise from transitions between highest occupied molecular orbitals (HOMO and HOMO − 1) and lowest unoccupied molecular orbitals (LUMO and LUMO +1). We found that in all of the molecules these four molecular orbitals are involved. Q-band in solution for most chlorins is described only through H → L and H − 1 → L + 1 transitions (in $\mathbf{4_c}$, L + 2 is also implied, and in $\mathbf{6_c}$, the four possible transitions appear with BLYP), whereas for most of the porphyrins the four transitions are involved (in $\mathbf{4_p}$, L + 2 is also implied).

Gouterman MOs in $\mathbf{2_p}$ and $\mathbf{3_p}$ are quite similar, but vinyl groups in $\mathbf{3_p}$ are somewhat conjugated with the π porphyrin system. This small enlargement of the π circuit is responsible for the enlargement of λ_Q. For $\mathbf{4_p}$, the H → L transition is the most important one in the description of the Q-band. It presents a small charge transfer toward two *meso*-carbons. It is interesting to note that the benzenic ring participates in the HOMO and LUMO, showing that this region is important in formation of the Q-band. Hence the calculations predict larger values of λ_Q in comparison with molecules unable to yield such large conjugation.

In the case of $\mathbf{5_p}$, there are two main electronic transitions, H − 1 → L and H → L + 1, the first one consisting of a small charge transfer from α- and β-carbon atoms toward the *meso*-carbon and unsubstituted N atoms, and the second of a transition from unsubstituted N atoms to the α- and β-carbon atoms of their pyrrole rings. For $\mathbf{6_c}$ the electronic transitions produce only a slight change from HOMO (or HOMO − 1) toward LUMO (or LUMO + 1) in the region of the pyrrole rings without internal H atoms. Some of the Gouterman MOs of these *meso* phenyl-substituted systems include phenyl MOs but they do not alter porphyrin skeleton MOs, so they do not really increase π.

Figure 2 shows that the transition H → L of $\mathbf{7_c}$ and $\mathbf{8_c}$ only implies a shift along the region of pyrrole rings without internal H atoms from the α-carbons toward the *meso*-C and N atoms. For the transition H − 1 → L + 1, a charge transfer occurs almost in the same way but in the opposite direction, a shift from the N atoms toward the α-carbons, always in pyrrole rings without internal H atoms.

3.3. Triplet Excited States. ***3.3.1. Molecular Structure.*** In this section the whole set of 16 molecules is analyzed. The first triplet state was studied as that responsible for the generation of singlet oxygen, which can produce the death of ill cells. In order to quantify the structural effect of the change in electronic state, from the singlet ground state to the first triplet excited state, we revised the same geometrical parameters analyzed previously for the ground state, which are also collected in Table 1 and in Supporting Information. Concerning dihedral angles it can be seen that the differences between the two electronic states range from 0.01° ($\angle C_1N_{21}N_{23}C_{14}$ of $\mathbf{1_p}$) to 12.9° ($\angle C_6N_{22}N_{24}C_{16}$ of $\mathbf{6_p}$) for the porphyrins and from 0.02° ($\angle C_1N_{21}N_{23}C_{11}$ of $\mathbf{1_c}$) to 17.9° ($\angle C_6N_{22}N_{24}C_{16}$ of $\mathbf{6_c}$ and $\mathbf{8_c}$) for the chlorins, indicating that the triplet state shows slight or significant changes in these molecules. In fact, the major differences occur for compounds with substitution at *meso*-carbon atoms: $\mathbf{5_p}/\mathbf{5_c}$, $\mathbf{6_p}/\mathbf{6_c}$, $\mathbf{7_p}/\mathbf{7_c}$, and $\mathbf{8_p}/\mathbf{8_c}$. Molecules with β-substitution, although less distorted in

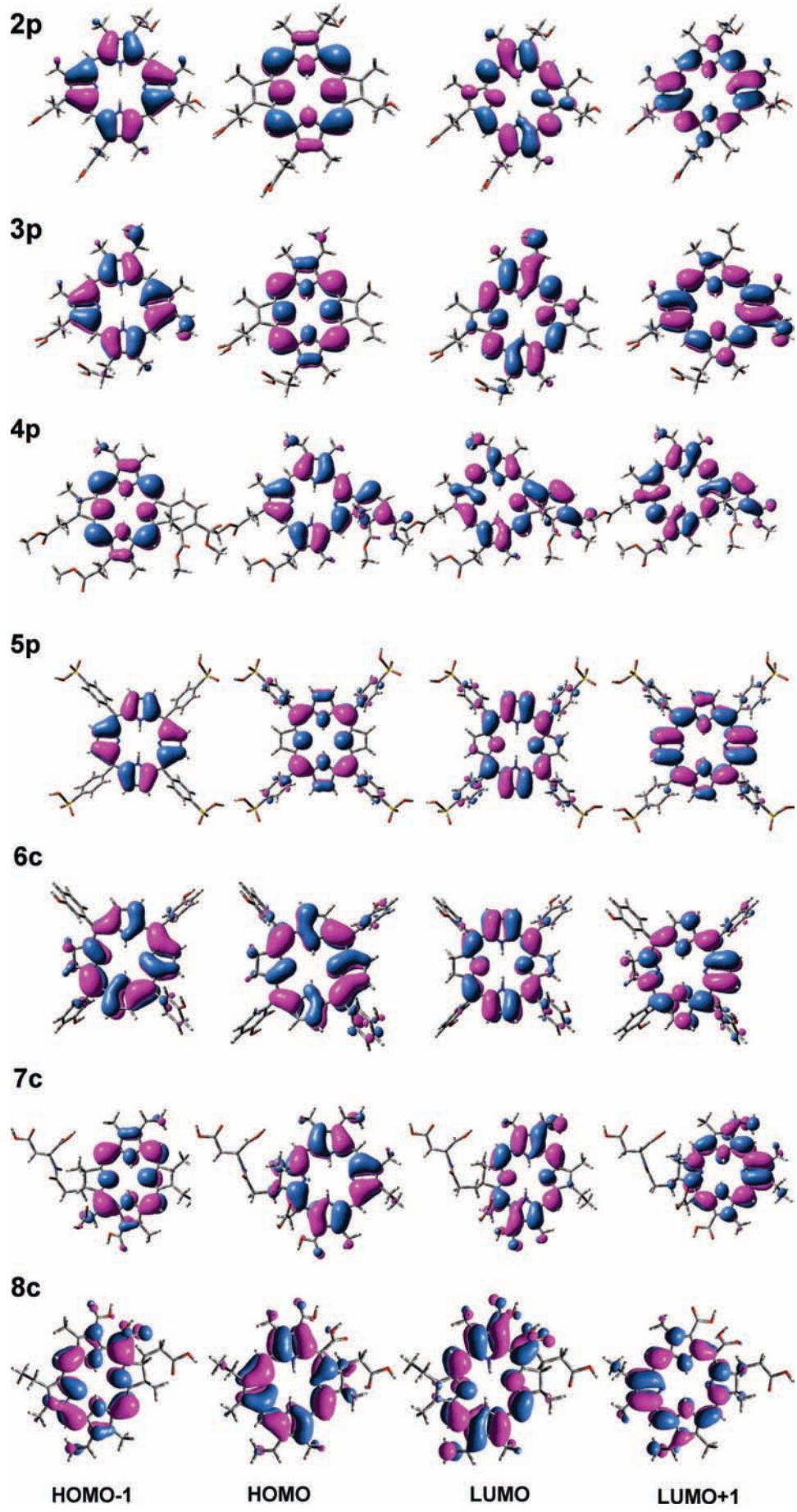

Figure 2. Molecular orbitals participating in the electronic transitions associated with Q-band, calculated at BLYP/6-31G(d) level in the gas phase.

TABLE 4: Energy Differences between First Excited Triplet State and Singlet Ground State[a]

	ΔE_{T-S_0}			ΔE_{T-S_0}	
porphyrin	gas phase	solution phase	chlorin	gas phase	solution phase
$\mathbf{1_p}$	1.68	1.72	$\mathbf{1_c}$	1.68	1.65
$\mathbf{2_p}$	1.62	1.67	$\mathbf{2_c}$	1.51	1.53
$\mathbf{3_p}$	1.62	1.65	$\mathbf{3_c}$	1.30	1.45
$\mathbf{4_p}$	1.38	1.38	$\mathbf{4_c}$	1.08	1.22
$\mathbf{5_p}$	1.60	1.63	$\mathbf{5_c}$	1.65	1.50
$\mathbf{6_p}$	1.52	1.60	$\mathbf{6_c}$	1.49	1.48
$\mathbf{7_p}$	1.65	1.68	$\mathbf{7_c}$	1.43	1.44
$\mathbf{8_p}$	1.51	1.49	$\mathbf{8_c}$	1.35	1.34

[a] ΔE_{T-S_0} was obtained at B3LYP/6-31G(d) level of calculation in the gas phase and in the solution phase (in methanol). All calculations were performed with Jaguar 6.0.

the triplet state, show greater twisting as the β-substituents become more complex, mainly $\mathbf{4_p}$. Concerning the distances between the *meso*-carbon atoms and between the N atoms of the pyrrole rings, the differences found between the ground and first excited triplet states are smaller than 0.1 Å for all the molecules. These results are included in Supporting Information.

3.3.2. Energy Change $T_1 \rightarrow S_0$. We also analyzed the energy difference between the ground-state and the first triplet excited state (ΔE_{T-S_0}), and the results obtained in gas and solution phases are shown in Table 4. An important characteristic of photosensitizer compounds is their ability to store energy in a triplet state that can be released when they decay to the ground state. This energy can be absorbed by the triplet molecular oxygen, yielding singlet oxygen. A value greater than 0.95 eV (22 kcal/mol) and smaller than 1.63 eV (37.5 kcal/mol) is required to be a good photosensitizer.[7] Overall, we observed that the values of ΔE_{T-S_0} increase when a solvent such as methanol is included in the calculation with the exception of $\mathbf{8_p}$, $\mathbf{5_c}$, $\mathbf{6_c}$, and $\mathbf{8_c}$, but changes are small except for $\mathbf{6_p}$ (0.08 eV), $\mathbf{4_c}$ (0.14 eV), and $\mathbf{3_c}$ (0.15 eV).

We found that all the studied systems release an amount of energy greater than the required 0.95 eV. Results in the gas phase predicted that $\mathbf{1_p}$, $\mathbf{7_p}$, $\mathbf{1_c}$, and $\mathbf{5_c}$ release energy greater than 1.63 eV. In solution, $\mathbf{4_p}$, $\mathbf{6_p}$, and $\mathbf{8_p}$ release energies lower than 1.63 eV and the same is true for all the chlorins except $\mathbf{1_c}$. Based on these results, it is clear that chlorin-like structures, excepting $\mathbf{1_c}$, can be considered better photosensitizers than porphyrin-like structures.

A comparison between analogous porphyrins and chlorins calculated in methanol solution shows that in all cases the emission energy from the triplet is minor in chlorins, suggesting that a reduction in a double bond of a pyrrole ring could change the properties of a compound, leading to increased photosensitizer capability.

4. Conclusions

The present work has shown that calculation of the electronic absorption spectra, along with emission energies from the first triplet excited state, allows us to deeply characterize several porphyrin and chlorin derivatives already reported in the literature and to propose new compounds that could have improved photosensitizing properties: in our proposal, substituted porphyrins and chlorins analogous to known ones.

In summary, we found the following: (a) TD-DFT yields satisfactory results at a moderate computational cost, and solvent effects on electronic spectra can be well described by the CPCM model. (b) *meso* substituents lead to greater geometry distortions than β-substituents in both porphyrins and chlorins and in both singlet and triplet states. (c) The presence of substituents in β positions provokes a red shift of λ_Q in both, porphyrins and chlorins and our calculations reproduce this trend. (d) A chlorin structure also shifts λ_Q to the red region in comparison with an analogous porphyrin structure. This fact was known for unsubstituted patterns and our study at BHANDHLYP/6-31+G(d) always predicts this trend for the eight couples considered in this work. (e) In methanol solution, $\mathbf{4_p}$, $\mathbf{6_p}$, and $\mathbf{8_p}$, along with all of the substituted chlorins, release appropriate energy to generate singlet oxygen when they decay from their first triplet excited state to the ground state. (f) Visudyne compounds, $\mathbf{4_p}$ and $\mathbf{4_c}$, seem to be the most appropriate for use in PDT among those studied in this work.

Acknowledgment. We acknowledge the financial support of Project FONDECYT (8010006 and 1060203) from CONICYT-CHILE, Spanish MEC (PCI2005-A7-0304) and the computational time provided by Project DICYT-USACH Apoyo Complementario. M.P. thanks FONDECYT (8010006) and DIGEGRA/USACH for a fellowship.

Supporting Information Available: Full electronic absorption spectra calculated in solution phase (explicit and continuum solvent model) with all exchange−correlation functionals used in this work on corresponding optimized molecular structures for the ground state (singlet); electronic absorption spectra calculated in the gas phase with BLYP functional; and optimized geometry for the first triplet excited state of all substituted porphyrin and chlorin structures. This material is available free of charge via the Internet at http://pubs.acs.org.

References and Notes

(1) Senge, M. O.; Fazekas, M.; Notaras, E. G. A.; Blau, W. J.; Zawadzka, M.; Locos, O. B.; Ni Mhuircheartaigh, E. M. *Adv. Mater.* **2007**, *19*, 2737–2774.

(2) Gupta, V. K.; Chauhan, D. K.; Saini, V. K.; Agarwal, S.; Antonijevic, M. M.; Lang, H. *Sensors* **2003**, *3*, 223–235.

(3) Lei, J.; Ju, H.; Ikeda, O. *Sensors* **2005**, *5*, 171–184.

(4) Castano, A. P.; Demidova, T. N.; Hamblin, M. R. *Photodiagn. Photodyn. Ther.* **2004**, *1*, 279–293.

(5) Castano, A. P.; Demidova, T. N.; Hamblin, M. R. *Photodiagn. Photodyn. Ther.* **2005**, *2*, 1–23.

(6) Castano, A. P.; Demidova, T. N.; Hamblin, M. R. *Photodiagn. Photodyn. Ther.* **2005**, *2*, 91–106 (review).

(7) Stemberg, E. D.; Dolphin, D. *Tetrahedron* **1998**, *54*, 4151–4202.

(8) Osterloh, J.; Vicente, M. G. *J. Porphyrins Phthlocyanines* **2002**, *6*, 305–324.

(9) Hilmey, D. G.; Abe, M.; Nelen, M. I.; Stilts, C. E.; Baker, G. A.; Baker, S. N.; Bright, F. V.; Davies, S. R.; Gollnick, S. O.; Oseroff, A. R.; Gibson, S. L.; Hilf, R.; Detty, M. R. *J. Med. Chem.* **2002**, *45*, 449–461.

(10) Pushpan, S. K.; Venkatraman, S.; Anand, V. G.; Sankar, J.; Parmeswaran, D.; Ganesan, S.; Chandrashekar, T. K. *Curr. Med. Chem.: Anti-Cancer Agents* **2002**, *2*, 187–207.

(11) Allison, R. R.; Downie, G. H.; Cuenca, R.; Hu, X.-H.; Childs, C. J. H.; Sibata, C. H. *Photodiagn. Photodyn. Ther.* **2004**, *1*, 27–42.

(12) Parmeswaran, D.; Pushpan, S. K.; Srinivasan, A.; Ravi Kumar, M.; Chandrashekar, T. K.; Ganesan, S. *Photochem. Photobiol.* **2003**, *78*, 487–495.

(13) Bonnet, R.; Martinez, G. *Tetrahedron* **2001**, *57*, 9513–9547.

(14) Nowis, D.; Makowski, M.; Stokłosa, T.; Legat, M.; Issat, T.; Gołb, J. *Acta Biochim. Pol.* **2005**, *52*, 339–352.

(15) Arad, O.; Gavaldá, A.; Rey, O.; Rubio, N.; Sánchez-García, D.; Borrell, J. I.; Teixidó, J.; Nonell, S.; Cañete, M.; Juarranz, A.; Villanueva, A.; Stockert, J. C.; Díaz Jiménez, P. J. *Afinidad* **2002**, *59* (500), 343–356.

(16) Calzavara-Pinton, P. G.; Venturini, M.; Sala, R. *J. Eur. Acad. Dermatol. Venereol.* **2007**, *21*, 293–302.

(17) Hasn, T.; Ortel, B.; Moor, A. C. E.; Pogue, B. W. Photodynamic Therapy of Cancer. In *Cancer Medicine*; Frei, H., Ed.; Dekker: Hamilton, Ontario, Canada, 2003; Chapt. 40.

(18) Friberg, E. G.; Cunderlkova, B.; Pettersen, E. O.; Moan, J. *Cancer Lett.* **2003**, *195*, 73–80.

(19) Banfi, S.; Caruso, E.; Caprioli, S.; Mazzagatti, L.; Canti, G.; Ravizza, R.; Gariboldia, M.; Montia, E. *Bioorg. Med. Chem.* **2004**, *12*, 4853–4860.

(20) Nyman, E. S.; Hynninen, P. H. *J. Photochem. Photobiol., B* **2004**, *73*, 1–28.

(21) Bruckner, C.; McCarthy, J. R.; Daniell, H. W.; Pendon, Z. D.; Ilagan, R. P.; Francis, T. M.; Ren, L.; Birge, R. R.; Frank, H. A. *Chem. Phys.* **2003**, *294*, 285–303.

(22) Quartarolo, A. D.; Russo, N.; Sicilia, E.; Lelj, F. *J. Chem. Theory Comput.* **2007**, *3*, 860–869.

(23) Cárdenas-Jirón, G. I.; Venegas, C.; López, R.; Menéndez, M. I. *J. Phys. Chem. A* **2008**, *112*, 8100–8106.

(24) Andzelm, J.; Rawlett, A. M.; Orlicki, J. A.; Snyder, J. F. *J. Chem. Theory Comput* **2007**, *3*, 870–877.

(25) Petit, L.; Quartarolo, A.; Adamo, C.; Russo, N. *J. Phys. Chem. B* **2006**, *110*, 2398–2404.

(26) Quartarolo, A. D.; Russo, N.; Sicilia, E. *Chem.—Eur. J.* **2006**, *12*, 6797–6803.

(27) Fukuda, H.; Casas, A.; Batlle, A. *Int. J. Biochem. Cell Biol.* **2005**, *37*, 272–276.

(28) Ichikawaa, K.; Takeuchia, Y.; Yonezawaa, S.; Hikitaa, T.; Kurohanea, K.; Nambab, Y.; Oku, N. *Cancer Lett.* **2004**, *205*, 39–48.

(29) Sailer, R.; Strauss, W. S. L.; Emmert, H.; Stock, K.; Steiner, R.; Schneckenburger, H. *Photochem. Photobiol.* **2000**, *71*, 460–465.

(30) Sasnouskia, S.; Zorinb, V.; Khludeyevb, I.; D'Hallewina, M. A.; Guillemina, F.; Bezdetnaya, L. *Biochim. Biophys. Acta* **2005**, *1725*, 394–402.

(31) Chen, J. Y.; Mak, N. K.; Yow, C. M. N.; Fung, M. C.; Chiu, L. C.; Leung, W. N.; Cheung, N. H. *Photochem. Photobiol.* **2000**, *72* (4), 541–547.

(32) Kobayashi, W.; Liu, Q.; Nakagawa, H.; Sakaki, H.; Teh, B. W.; Matsumiya, T.; Yoshida, H.; Imaizumi, T.; Satoh, K.; Kimura, H. *Oral Oncol.* **2006**, *42*, 46–50.

(33) Dube, A.; Sharma, S.; Gupta, P. K. *Oral Oncol.* **2006**, *42*, 77–82.

(34) (a) Lee, C.; Yang, W.; Parr, R. G. *Phys. Rev. B* **1988**, *37*, 785–789. (b) Miehlich, B.; Savin, A.; Stoll, H.; Preuss, H. *Chem. Phys. Lett.* **1989**, *157*, 200–206. (c) Becke, A. D. *J. Chem. Phys.* **1993**, *98*, 5648–5652.

(35) Jaguar, version 7.5; Schrodinger, LLC, New York, 2008.

(36) (a) Tannor, D. J.; Marten, B.; Murphy, R.; Friesner, R. A.; Sitkoff, D.; Nicholls, A.; Ringnalda, M.; Goddard, W. A., III; Honig, B. *J. Am. Chem. Soc.* **1994**, *116*, 11875–11882. (b) Marten, B.; Kim, K.; Cortis, C.; Friesner, R. A.; Murphy, R.; Ringnalda, M.; Sitkoff, D.; Honig, B. *J. Phys. Chem.* **1996**, *100*, 11775–11788.

(37) Stratmann, R. E.; Scuseria, G. E.; Frisch, M. J. *J. Chem. Phys.* **1998**, *109*, 8218–8224.

(38) Bauernschmitt, R.; Ahlrichs, R. *Chem. Phys. Lett.* **1996**, *256*, 454–464.

(39) Casida, M. E.; Jamorski, C.; Casida, K. C.; Salahub, D. R. *J. Chem. Phys.* **1998**, *108*, 4439–4449.

(40) Frisch, M. J.; Trucks, G. W.; Schlegel, H. B.; Scuseria, G. E.; Robb, M. A.; Cheeseman, J. R.; Montgomery, J. A., Jr.; Vreven, T.; Kudin, K. N.; Burant, J. C.; Millam, J. M.; Iyengar, S. S.; Tomasi, J.; Barone, V.; Mennucci, B.; Cossi, M.; Scalmani, G.; Rega, N.; Petersson, G. A.; Nakatsuji, H.; Hada, M.; Ehara, M.; Toyota, K.; Fukuda, R.; Hasegawa, J.; Ishida, M.; Nakajima, T.; Honda, Y.; Kitao, O.; Nakai, H.; Klene, M.; Li, X.; Knox, J. E.; Hratchian, H. P.; Cross, J. B.; Bakken, V.; Adamo, C.; Jaramillo, J.; Gomperts, R.; Stratmann, R. E.; Yazyev, O.; Austin, A. J.; Cammi, R.; Pomelli, C.; Ochterski, J. W.; Ayala, P. Y.; Morokuma, K.; Voth, G. A.; Salvador, P.; Dannenberg, J. J.; Zakrzewski, V. G.; Dapprich, S.; Daniels, A. D.; Strain, M. C.; Farkas, O.; Malick, D. K.; Rabuck, A. D.; Raghavachari, K.; Foresman, J. B.; Ortiz, J. V.; Cui, Q.; Baboul, A. G.; Clifford, S.; Cioslowski, J.; Stefanov, B. B.; Liu, G.; Liashenko, A.; Piskorz, P.; Komaromi, I.; Martin, R. L.; Fox, D. J.; Keith, T.; Al-Laham, M. A.; Peng, C. Y.; Nanayakkara, A.; Challacombe, M.; Gill, P. M. W.; Johnson, B.; Chen, W.; Wong, M. W.; Gonzalez, C.; Pople, J. A. Gaussian 03, revision D.01; Gaussian, Inc.: Wallingford, CT, 2004.

(41) (a) Barone, V.; Cossi, M. *J. Phys. Chem. A* **1998**, *102*, 1995–2001. (b) Cossi, M.; Rega, N.; Scalmani, G.; Barone, V. *J. Comput. Chem.* **2003**, *24*, 669–681.

(42) Sundholm, D. *Phys. Chem. Chem. Phys.* **2000**, *2*, 2275–2281.

(43) Parusel, A. B. J.; Grimme, S. *J. Porphyrins Phthalocyanines* **2001**, *5*, 225–232.

(44) Parusel, A. B. J.; Ghosh, A. *J. Phys. Chem. A* **2000**, *104*, 2504–2507.

(45) Grimme, S.; Waletzke, M. *J. Chem. Phys.* **1999**, *111*, 5645–5655.

(46) van Gisbergen, S. J. A.; Rosa, A.; Ricciardi, G.; Baerends, E. J. *J. Chem. Phys.* **1999**, *111*, 2499–2506.

(47) Kitao, O.; Ushiyama, H.; Miura, N. *J. Chem. Phys.* **1999**, *110*, 2936–2946.

(48) Serrano-Andrés, L.; Merchán, M.; Rubio, M.; Roos, B. O. *Chem. Phys. Lett.* **1998**, *295*, 195–203.

(49) Tokita, Y.; Hasegawa, J.; Nakatsuji, N. *J. Phys. Chem. A* **1998**, *102*, 1843–1849.

(50) Gwaltney, S. R.; Bartlett, R. J. *J. Chem. Phys.* **1998**, *108*, 6790–6798.

(51) Hasegawa, J.; Ozeki, Y.; Ohkawa, K.; Hada, M.; Nakatsuji, H. *J. Phys. Chem. B* **1998**, *102*, 1320–1326.

(52) Nooijen, M.; Bartlett, R. J. *J. Chem. Phys.* **1997**, *106*, 6449–6455.

(53) Nakatsuji, H.; Hasegawa, J.; Hada, M. *J. Chem. Phys.* **1996**, *104*, 2321–2329.

(54) Roos, B. O.; Fülscher, M. P.; Malmqvist, P.-A.; Merchán, M.; Serrano-Andrés, L. Theoretical studies of electronic spectra of organic molecules. In *Quantum Mechanical Electronic Structure Calculations with Chemical Accuracy*; Langhoff, S. R., Ed.; Kluwer Academic: Dordrecht, The Netherlands, 1995; p 357.

(55) Baraldi, I.; Carnevali, A.; Ponterini, G.; Vanossi, D. *J. Mol. Struct. (THEOCHEM)* **1995**, *333*, 121–133.

(56) Merchán, M.; Ortí, E.; Roos, B. O. *Chem. Phys. Lett.* **1994**, *226*, 27–36.

(57) Yamamoto, Y.; Noro, T.; Ohno, K. *Int. J. Quantum Chem.* **1992**, *42*, 1563–1575.

(58) Foresman, J. B.; Head-Gordon, M.; Pople, J. A.; Frisch, M. J. *J. Phys. Chem.* **1992**, *96*, 135–149.

(59) Baker, J. D.; Zerner, M. C. *Chem. Phys. Lett.* **1990**, *175*, 192–196.

(60) Nagashima, U.; Takada, T.; Ohno, K. *J. Chem. Phys.* **1986**, *85*, 4524–4529.

(61) Hasegawa, J.; Kimura, T.; Nakatsuji, H. *J. Porphyrins Phthalocyanines* **2005**, *9*, 305–315.

(62) Hashimoto, T.; Choe, Y.-K.; Nakano, H.; Hirao, K. *J. Phys. Chem. A* **1999**, *103*, 1894–1904.

(63) Edwards, L.; Dolphin, D. H.; Gouterman, M.; Adler, A. D. *J. Mol. Spectrosc.* **1971**, *38*, 16–32.

(64) (a) Smith, K. M. *Porphyrins and Metalloporphyrins*; Elsevier: Amsterdam, 1975. (b) Jarrett, S. G.; Boulton, M. E. *J. Photochem. Photobiol., B* **2001**, *64*, 144–161. (c) Sagun, E. I.; Zenkevich, E. I.; Knyukshto, V. N.; Shulga, A. M.; Starukhin, D. A.; von Borczyskowski, C. *Chem. Phys.* **2002**, *275*, 211–237.

(65) Gouterman, M. In *The Porphyrins, Vol. III, Part A: Physical Chemistry*; Dolphin, D., Ed.; Academic Press: New York, 1978.

(66) Gouterman, M. *J. Mol. Spectrosc.* **1961**, *6*, 138–163.

(67) Gouterman, M.; Wagnière, G. H.; Snyder, L. C. *J. Mol. Spectrosc.* **1963**, *11*, 108–127.

JP804350N